Journal of Modern Processes in Manufacturing and Production, Volume 9, No. 2, Spring 2020

DOR: 20.1001.1.27170314.2020.9.2.1.5

Research Paper

Numerical Simulation of Homogeneous, Two and Three Lattice Layers Scaffolds with Constant Density

Hamid Reza Khanaki[1], Sadegh Rahmati[2*], Mohammad Nikkhoo[2*], Mohammad Haghpanahi[3], Javad Akbari[4]

[1]Department of Mechanical Engineering, Science and Research Branch, Islamic Azad University, Tehran, Iran

[2]Department of Biomedical Engineering, Science and Research Branch, Islamic Azad University, Tehran, Iran

[3]Biomechanics Group, Department of Mechanical Engineering, Iran University of Science and Technology, Tehran, Iran

[4]Department of Mechanical Engineering, Sharif University of Technology, Tehran, Iran

[*]Email of Corresponding Authors: srahmati@srbiau.ac.ir, m.nikkhoo@srbiau.ac.ir

Received: March7, 2020; Accepted: May 20, 2020

Abstract

Advances in the additive manufacturing technology have led to the production of complex microstructures with unprecedented accuracy and due todesigning an effective implant is a major scientific challenge in bone tissue regeneration and bone growth. In this research, titanium alloy cylindrical scaffolds with three-dimensional architectures have been simulated and compared for curing partial bone deficiencies. The cylindrical networks in the scaffold (outer diameter 15 and length 30 millimeters) were designed in 36 different convergent, two-layer and three-layer types with 50% and 70% porosity. In all the samples, outer layers were denser than the inner layers. Mechanical characteristics of these scaffolds have been determined by simulating uniform compression load. The stress-strain curve of the samples showed that Young's modulus and yield stress in the scaffolds with constant porosity were related to a unit-cell and the two-layer scaffolds, without changing Young's modulus, had higher yield stress. This advantage was more significant in high-density scaffolds.

Keywords

Bone scaffold, Implant, Additive Manufacturing, Numerical Analysis

1. Introduction

One of the outlooks of the orthopedic surgery is metallic bone scaffolds and implants, inspired by a form of life which repeats biomechanical characteristics and the host's natural bone structure. The proper design of the scaffolds is a key factor for desirable clinical results. An ideal metallic implant, similar to natural bone, must at least be porous to an extent and should have parts with controlled navigation cues. Despite recent progresses in biology, designing and building such scaffolds is still a challenge [1].

Using porous scaffolds as a bone replacement for curing complete bone damages is problematic, often because of limited bone tissue penetration and angiogenesis process, especially in the inner

area [2, 3]. Designing an empty middle space for imitating the tall bone structure has been proposed and shown in previous studies, which eases the bone tissue penetration and angiogenesis [2, 4].

Producing implants with graded porosity from hydroxyapatite substance has been done and has shown that high porosity part allows proper and quick bone growth and low porosity part endures the mechanical stress.

Becker and Pompe reported that graded substances give the required strength to the implant to resist against physiological load and the graded porosity structure optimizes the substances' response to external loading, also this similar advantage can be useful for artificial bone implant [6, 7].

Recently due to the presence and progress of additive manufacturing technology, which enables us to build desirable complex forms with micro and even nanoscales, the interest for building cell scaffolds with proper mechanical characteristics has increased. Cube [8-10], truncated cube [11], rhombic dodecahedron [12-15], truncated cuboctahedron [14], Kelvin cell [16, 17], rhombicuboctahedron [18], 3D-kagome [19], pyramid [20], diamond [21, 22], truncated octahedron [23–25] are open-lattice network's cell morphologies, which have been studied more.

A cell scaffold, which is exclusive to biological applications, has been recently discussed. In this research two and three-layer titanium alloy (Ti6Al4V) made scaffolds, with electron beam melting (EBM), have been successfully made and compared [26]. This research showed that titanium made scaffolds with graded porosity, in addition to reducing Young's modulus, compared to dens alloy, had significant ductility.

Mechanical characteristics of biogenic substances, in addition to unit-cell type and its measurements, depends on a great number of layers. Therefore, the unit-cell type, measurements, and the number of layers can be changed, and the mechanical cues can be optimized. In most cases, mechanical characteristics of the porous scaffolds play an important role in adjusting the tissue regeneration function. On one hand, the biogenic porous substances must be resistant enough to support tissue regeneration. On the other hand, they must have too high Young's modulus, because it prevents the mechanical load from the regenerated tissue, which is essential for its regeneration.

Optimal design of the porous scaffolds requires tools that can be used for predicting mechanical cues, acquired from each set of parameters. There are three experimental, numerical and analytical methods that can be used for predicting mechanical characteristics of the porous biogenic substances. The experimental approach is probably more precise but requires producing and mechanically testing a great number of samples. It may be suitable for testing the final optimized design but is unacceptable for the process of optimizing the designs, regarding which many alternative designs may need assessment. Numerical and analytical approaches do not require production and mechanical test of many samples, therefore, they are suitable for the process of optimizing the design. The numerical approach's advantage over the analytical approach is the possibility of building models that are better than porous biogenic substances. For example, the deficiencies from the production process can be executed in numerical models, whereas they cannot be easily taken into account in the analytical approach.

The majority of the researches have focused on regular convergent porosities, and researches regarding multilayer scaffolds have been less focused on. The aim of this research was examining the effective factors on the mechanical characteristics of the multilayer scaffolds with constant density.

2. Research Method

Since a porous scaffold is used as a replacement for biogenic substances, compression load is utilized vastly as a loading method; at the first stage, five types of two and three-layer cylindrical scaffolds made of titanium alloy under compression load were studied according to the data from previous researches (Figure 1). Mechanical characteristics of the scaffolds were determined and compared with experimental results through doing a numerical simulation of uniform compression load test. Then after verifying the numerical method, 36 types of convergent two and three-layer cylindrical scaffolds (outer diameter 15 and length 30 mm) with 50 and 70% porosity and different unit-cell form, made from titanium alloy were designed and the mechanical characteristics of the scaffolds were determined through a numerical simulation, and the effects of the strut's diameter (unit-cell), number of layers and unit-cell from on mechanical characteristics were evaluated.

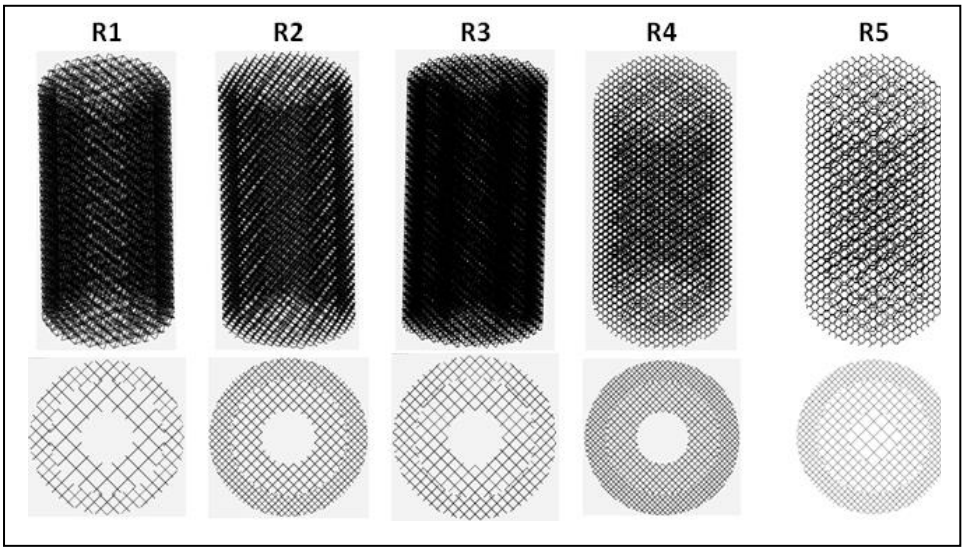

Figure 1.Samples of two layers (R1, R2, R3, R4) and three layers (R5) of scaffolds

3. Numerical Simulation of Multilayer Cell Scaffold

3.1 Simulation of the Scaffolds, Designed by Previous Researchers

To verify the results of the simulation in ANSYS, five tests of the multilayer scaffolds, under compression load [26] were modeled in the software and the experimental results from the previous researchers were compared with the results from the simulation using finite element method (Figure 2).

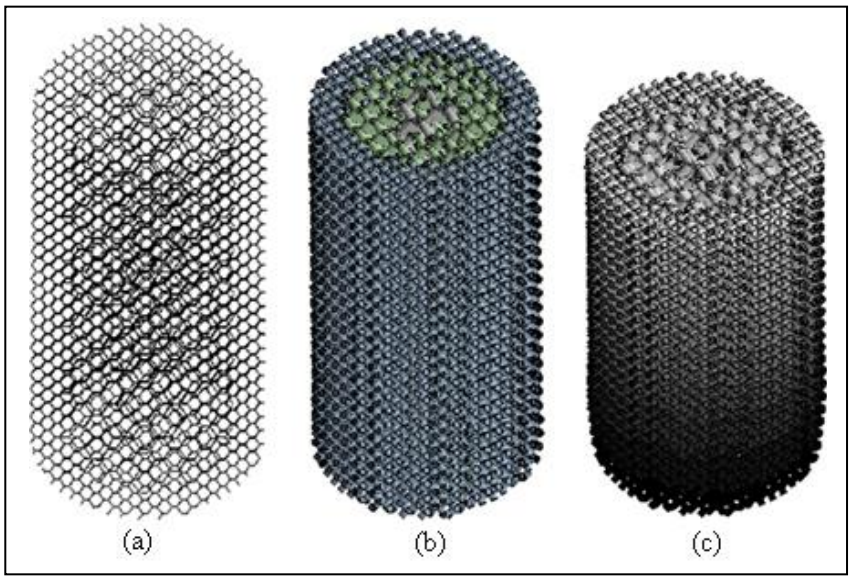

Figure2. Three-layer scaffold before ((a) wireframe, (b) solid) and (c) after loading

The characteristics of the five two-layer and three-layer cylindrical scaffolds with the two body-centered cubic (BCC) and diamond unit-cell forms (Figure 3) have been presented in Table 1.The difference between percentage of experimental and numerical porosity of R3-B and R4-D scaffolds could be due to incomplete powder removal in these scaffolds in the small size unit cell of the scaffolding.

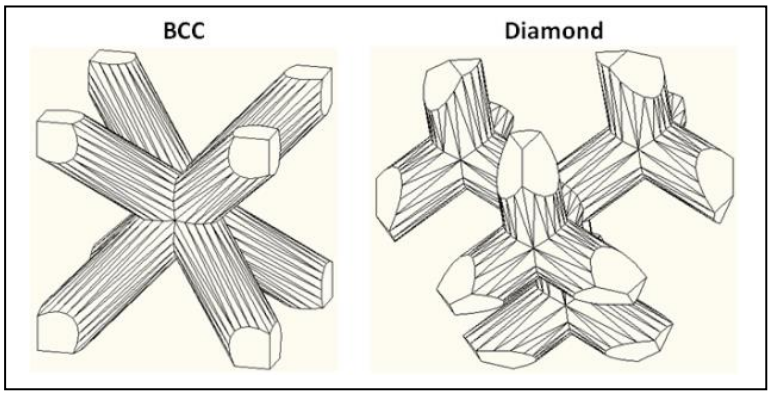

Figure3. BCC (left), Diamond (right) scaffold unit cells

Table1.The geometric and porosity percentage of the scaffolds

scaffold	Inner diameter (5 mm)	Middle diameter (11 mm)	Outer diameter (15 mm)	experimental porosity[26] %	Modeling porosity %
R1-B	Open hole	BCC-2	BCC-1.25	64	59
R2-D	Open hole	D-2	D-1.25	65	62
R3-B	Open hole	BCC-1.25	BCC-1	22	34
R4-D	Open hole	D-1.25	D-1	21	41

R5-D	D-3	D-2	D-1.25	65	65

In the numerical simulation with ANSYS software for rod structures like the porous structures of the current research, linear elements are usually more cost-effective, compared to flat and volume elements. Using linear elements, building and analyzing big porous structures, consisting of a great number of struts, does not require too many computational endeavors [27]. Since the struts in open-lattice cell structures are usually under axial and bendingload, beam elements with two or three nodes with program control can be considered as the best choice for this.
struts are connected rigidly at the tops. Since the analysis of this study was in a completely elastic area, it was assumed that the substance was linear elastic.
In all simulated porous structures, to reduce the effect of boundary conditions on the scaffold's mechanical cues, the nodes on the lower plane of the network structure were limited to three directions (x,y,z=0) and the nodes on the upper side of the scaffold were moved towards the axis of the scaffold in a way that the porous structure moved until 0.1% of compressive strain. The scaffold's axial stress was achieved by dividing axial force on the scaffold's cross-section and then elastic modulus was easily acquired by dividing axial stress, applied on the axial strain. By achieving maximum stress in the porous structure and then dividing that with titanium alloy yield stress, yield strain of the porous structure was found and by multiplying the yield strain with the scaffold's Young's modulus, the scaffold's yield stress was determined.
The mechanical characteristics of titanium alloy (Ti6Al4V), which was used in the simulations, were (Table 2):

Table2.Mechanical properties of titanium alloy [26]

Properties	Symbol	Value
Young's modulus	E_s	114 GPa
Poisson's ratio	N_s	0.37
Yield strength	σ_{ys}	920 MPa

3.2 Designing and Stimulating Multilayer Scaffold with Constant Density

Many articles, focusing on optimizing the scaffold's network design, have been published regarding the dependence of the biological cell's penetration on the scaffold, the tissue and vessel growth and also the transferring of desirable amounts of nutrition to the regenerating tissue [1, 28]. The effect of the size of the outlets on the tissue's growth is controversial, but 100-900 micrometer cavities for having good bone growth have been reported in articles [1]. Also according to the fact that many articles have proven the biocompatibility of the titanium alloy scaffolds [29, 30], in this research, titanium alloy made scaffolds with mechanical characteristics mentioned in the Table 2were designed. For modeling, first, cylindrical scaffolds with 15 mm diameter and 30 mm length were designed, using AutoCAD software (Figure 4).

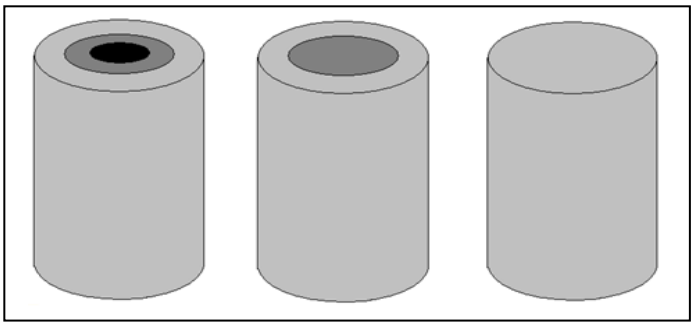

Figure 4. One-layer, two-layer and three-layer cylindrical moldings

Then primary cylindrical structures were filled in convergent, two-layer and three-layer forms, by the produced networks of three unit-cell forms of BCC, diamond, and cubic (Figure 5) with calculated measurements in a way that the constant porosity 50% and 70% could be achieved. The research focused on multilayer networks with unit-cells that were not complex. The used unit-cells were asymmetrical and their size was the same in all three dimensions; this size is called the network cell size.

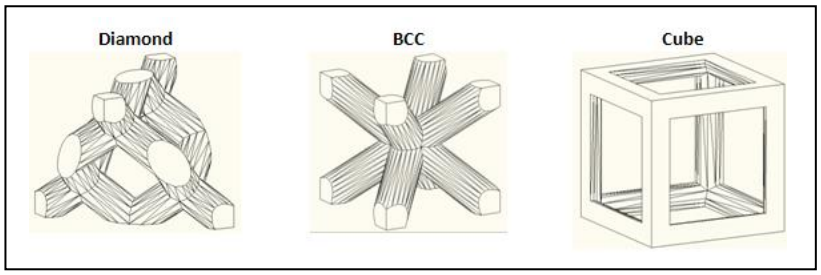

Figure 5. Three unit-cell forms (from right) of cubic, BCC and diamond

Assuming an equal cross-section for each layer in two-layer and three-layer scaffolds, the unit-cell size was specified in a way that 50% and 70% porosity was achieved (Table 3).

Table3. The layers' porosity percentage in scaffolds with 50% and 70% porosity

70% porosity			
Scaffold type	Porosity percentage of each layer		
Single layer		70%	
double layers	55%		85%
Three layers	55%	70%	85%
50% porosity			
Scaffold type	Porosity percentage of each layer		
Single layer		50%	
double layers	25%		75%
Three layers	25%	50%	75%

In the current research, the effects of the unit-cell, number of layers and the unit-cell strut diameter parameters on Young's modulus and yield stress of the bone scaffolds were examined. Three surfaces, unit-cell forms and layers and also two different strut diameters were used. Finally, by analyzing the data, the effective factors on Young's modulus and yield stress were determined.
In this article, scaffolds were designed through the full factorial design method. Full factorial design requires more time, compared to other methods, because of examining every possible state. However, since the aim of this study was the precise examination of the tests, this method has been used in designing. Minitab software has been used for designing the tests and analyzing the data. In designing the test, according to previous researchers' research, the most effective parameters in bone structures and their surfaces were chosen [26]. The number of layers and unit-cell form of each in three layers and the strut's diameter parameter in two layers were considered as the input parameters, and Young's modulus and compressive stress were considered as the most important output responses. In designing the scaffold, three factors were examined and for each of these factors, according to Table 4, the amounts of levels of changes were determined.

Table4. Factors and Taguchi's method surfaces

factor	Level (1)	Level (2)	Level (3)
Number of layers	1	2	3
Struts diameter	0.5 mm	0.75 mm	-
Cell shape	Cube	BCC	Diamond

Figure 6 and Table 5 show the convergent, two-layer and three-layer scaffolds with 70% porosity. Figure 7 and Table 6 show the convergent, two-layer and three-layer scaffolds with 50% porosity, which has been designed through full factorial design method.

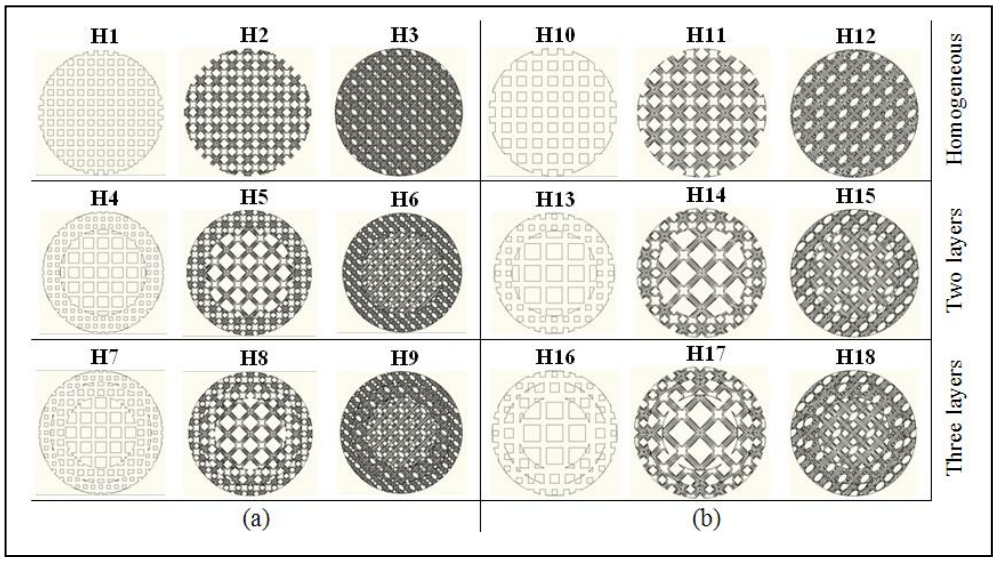

Figure 6. Designed scaffolds with 70% porosity a)0.5 mm, b)0.75 mm

Table5. Scaffolds designed with 70% porosity

scaffold	Struts diameter	Number of layers	Cell shape	Size unit cell)mm(		
H1	0.5	1	Cube	1.2		
H2	0.5	1	BCC	1.85		
H3	0.5	1	Diamond	1.75		
H4	0.5	2	Cube	Out 0.95		In 1.8
H5	0.5	2	BCC	Out 1.45		In 2.75
H6	0.5	2	Diamond	Out 1.35		In 2.7
H7	0.5	3	Cube	Out 0.95	Mid 1.2	In 1.8
H8	0.5	3	BCC	Out 1.45	Mid 1.85	In 2.75
H9	0.5	3	Diamond	Out 1.35	Mid 1.75	In 2.7
H10	0.75	1	Cube	1.8		
H11	0.75	1	BCC	2.75		
H12	0.75	1	Diamond	2.7		
H13	0.75	2	Cube	Out 1.4		In 2.7
H14	0.75	2	BCC	Out 2.15		In 4.15
H15	0.75	2	Diamond	Out 2.1		In 4.05
H16	0.75	3	Cube	Out 1.4	Mid 1.8	In 2.7
H17	0.75	3	BCC	Out 2.15	Mid 2.75	In 4.15
H18	0.75	3	Diamond	Out 2.1	Mid 2.7	In 4.05

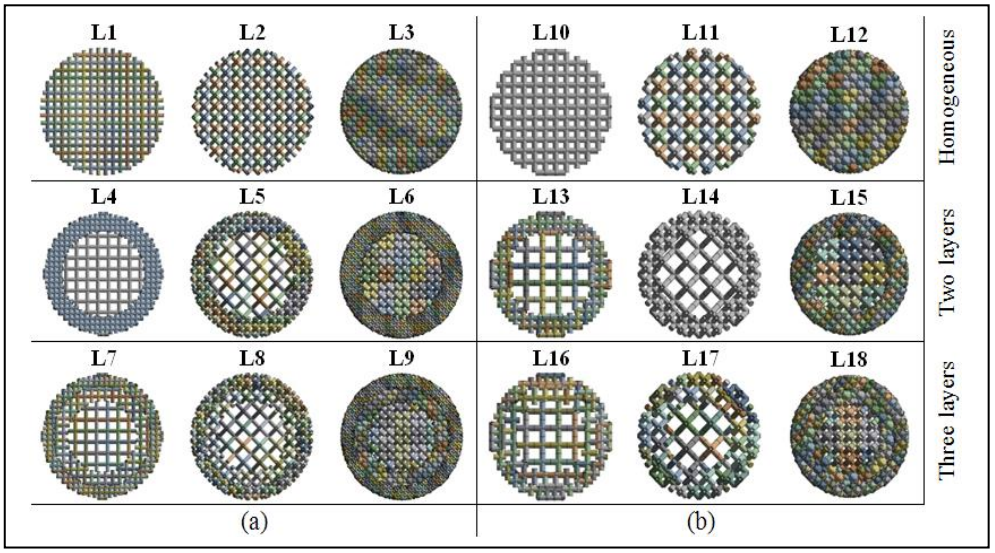

Figure 7. Scaffolds designed with 50% porosity a) 0.5 mm, b) 0.75 mm

Table 6. Scaffolds designed with 50% porosity

scaffold	Struts diameter	Number of layers	Cell shape	Size unit cell)mm(		
L1	0.5	1	Cube	0.881		
L2	0.5	1	BCC	1.35		
L3	0.5	1	Diamond	1.26		
L4	0.5	2	Cube	Out 0.65		In 1.354
L5	0.5	2	BCC	Out 1		In 2.07
L6	0.5	2	Diamond	Out 0.88		In 2
L7	0.5	3	Cube	Out 0.65	Mid 0.881	In 1.354
L8	0.5	3	BCC	Out 1	Mid 1.35	In 2.07
L9	0.5	3	Diamond	Out 0.88	Mid 1.26	In 2
L10	0.75	1	Cube	1.32		
L11	0.75	1	BCC	2.02		
L12	0.75	1	Diamond	1.89		
L13	0.75	2	Cube	Out 0.97		In 2.03
L14	0.75	2	BCC	Out 1.5		In 3.1
L15	0.75	2	Diamond	Out 1.31		In 3
L16	0.75	3	Cube	Out 0.97	Mid 1.32	In 2.03
L17	0.75	3	BCC	Out 1.5	Mid 2.02	In 3.1
L18	0.75	3	Diamond	Out 1.31	Mid 1.89	In 3

4. Results and Discussion

4.1 Comparing the Experimental Results with Numerical Simulation Results

The comparison of numerical and experimental Young's modulus results have been shown in Figure 8. The highest Young's modulus in both methods was found in the R4 sample. Also according to lower porosity in R3 and R4 scaffolds, mechanical characteristics showed an increase.

The graded titanium alloy scaffold structure that was examined in this study, showed a significant reduction in Young's modulus, compared to the dense alloy, which led to a significant reduction in stress-shielding.

Lower Young's modulus in experimental results can be caused by deficiencies in network structure's geometry and also low-quality production of the struts, forming the scaffold.

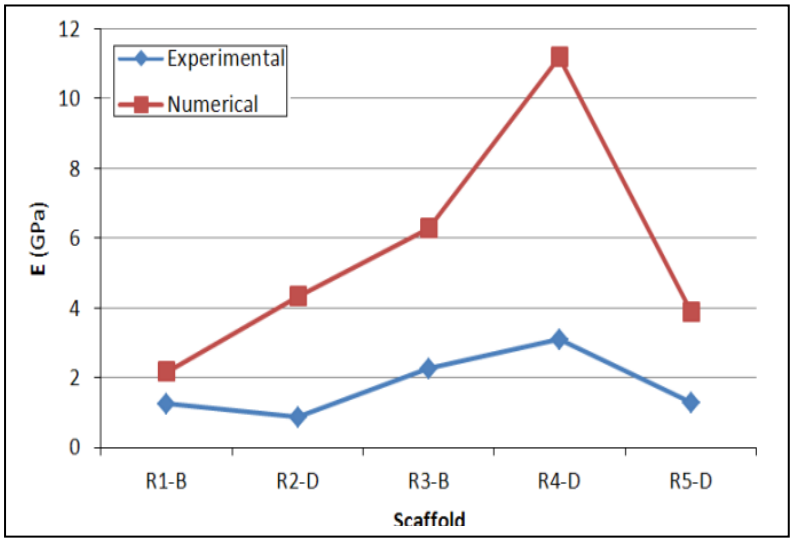

Figure8.Comparison between experimental and numerical Young's modulus of multilayer scaffolds

The comparison of experimental and numerical yield stress results have been shown in Figure 9. They showed that the scaffolds' micro-architectures changed their mechanical cues. The lowest yield stress in experimental results was in the R2 scaffold with 32 MPa diamond cell and 54 MPa in R1 scaffold with BCC cell in numerical results.

This difference can be caused by the production deficiencies, like free link, powder particles with incomplete melting, which was provided in the electronic microscope scan after the break (Figure 8 in reference [26]).

The highest yield stress in all three methods was in the R4 scaffold with a diamond cell.

Porous scaffolds include three definite parts in the stress-strain curve. Linear part (elastic), plateau phase (non-linear) and cumulative order phase (non-linear). But in the R3 scaffold's stress-strain curve in the experimental method, none of the stress regions were visible and the plateau stress for this scaffold increased gradually with compression increasing, which can be caused by probable existence of incompletely picked powder in dense networks' layers. Therefore, the yield stress has not been reported for this scaffold in the experimental method.

Yield stress reduction in the experimental results can be caused by deficiencies in the network structure's geometry and the low-quality of the production of struts forming the scaffold.

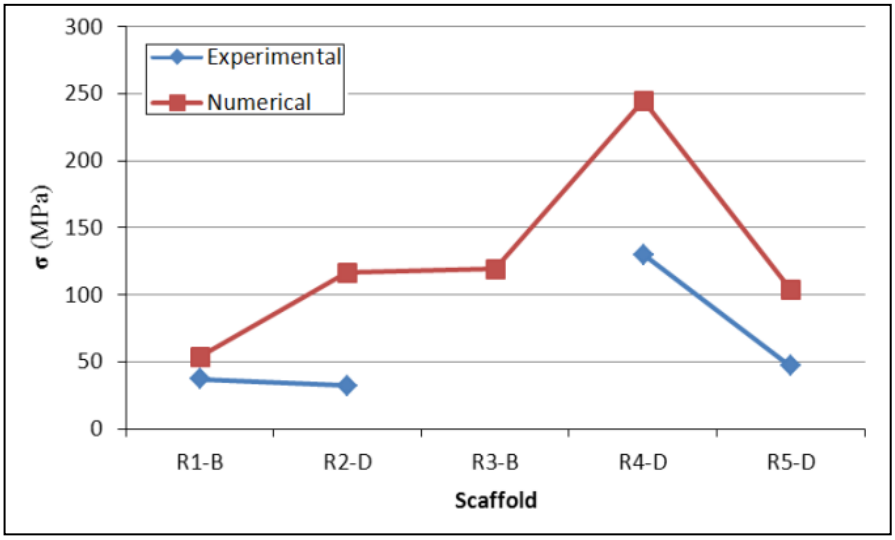

Figure9. Comparison of experimental and numerical results of multilayer scaffolds' yield strength

According to the aforementioned items, the proper conformity between numerical modeling results and experimental findings showed the ANSYS software's high capability of modeling multilayer scaffolds.

4.2 Young's Modulus of the Scaffolds with Constant Density

Young's modulus of scaffolds with 50% and 70% porosity has been shown in Figure 10. In the aforementioned figure, dm, Ln represents the strut's diameter (m) and the number of layers (n).

As expected, with increasing density in scaffolds with the same unit-cell, Young's modulus has increased and also because of cubic unit cell's navigation towards loading, Young's modulus's maxima has occurred in this type of scaffolds. The Young modulus's range for scaffolds with 70% porosity was1.08 – 18.66 GPa and having 50% porosity was 3.06 – 35.42 GPa.

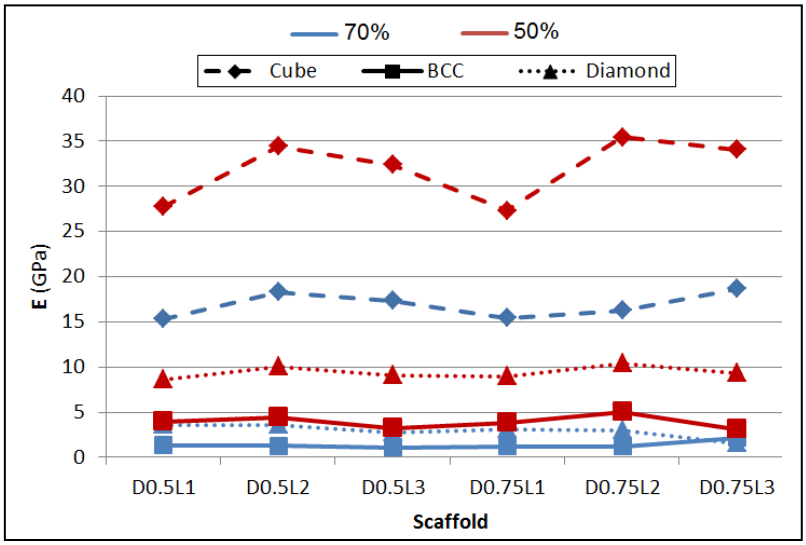

Figure10. Comparison of Young's modulus in scaffolds with 50% and 70% porosity

The analysis results of Young's modulus with 50% and 70% porosity have been presented in Figure 11. These results showed that Young's modulus of the scaffolds had less relation with the number of layers and the unit-cell strut diameter, and the most effective factor on Young's modulus of scaffolds was the unit-cell form. Therefore, it can be concluded that in scaffolds with similar unit-cell, according to Gibson-Ashby graph, porosity percentage determined the mechanical characteristics of the scaffold.

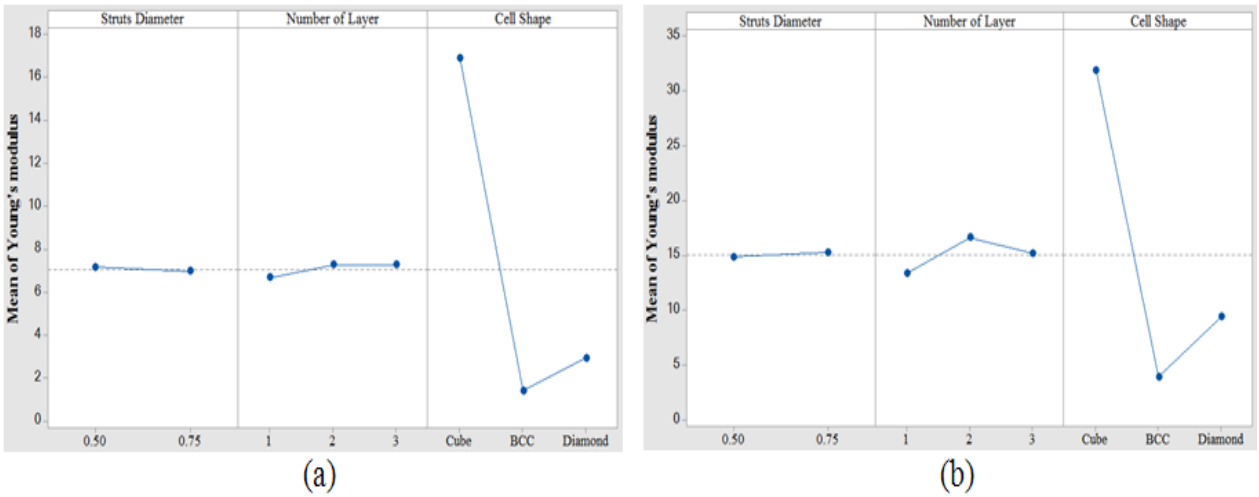

Figure 11. Young's modulus analysis in scaffolds with a) 70% porosity and b) 50% porosity

Figure 11 also shows that Young's modulus's maxima occurred in cubic unit-cell and Young's modulus's minima were in BCC unit-cell, which can be caused by low BCC unit-cell density, compared to the diamond.

Also increasing the number of layers caused Young's modulus to increase, and by reducing the porosity, the Young modulus's maxima has occurred in the two-layer scaffold, which can be caused because of the reduction in the number of free nodes in the layers' intersection because of higher unit cells` density in scaffolds with lower porosity.

4.3 Yield Strength in Scaffolds with Constant Density

The implant's biogenic substances must be strong enough in yield strength to be able to transfer the mechanical load without a big change in the form, which can endanger the implant's stability [31].

Figure 12 shows the yield strength results in scaffolds with 50% and 70% porosity.

The yield strength range for scaffolds with 70% porosity was 31.12 – 148.19 MPa, and for scaffolds with 50% porosity, it was 67.2 – 277.14 MPa.

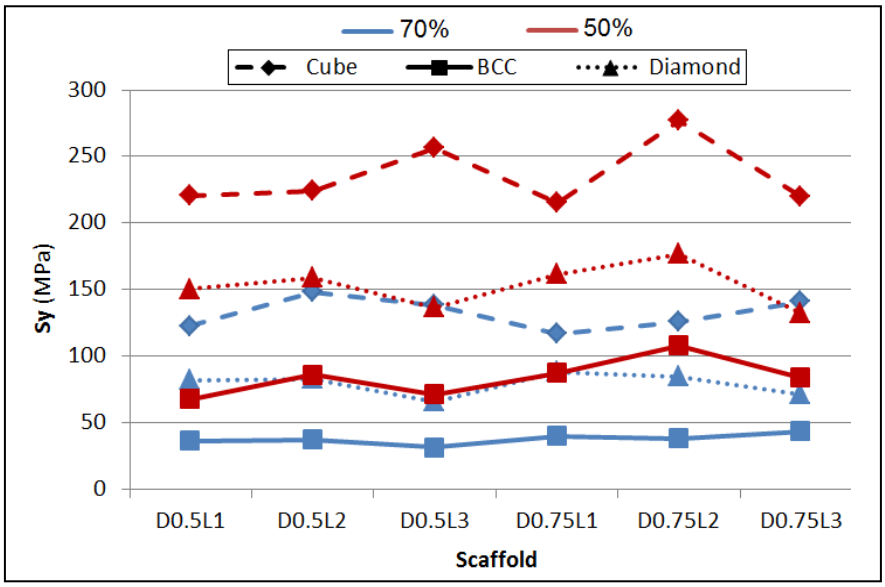

Figure12.Yield strength comparison in scaffolds with 50% and 70% porosity

Yield strength analysis results have been presented in Figure 13. These results showed that yield strength in scaffolds, depended less on the number of layers and the unit-cell strut's diameter, and the only effective factor on the scaffold's yield strength was the unit-cell form. It also showed that the highest yield strength in scaffolds occurred in two-layer scaffolds. Also, this advantage was more significant in high-density scaffolds.

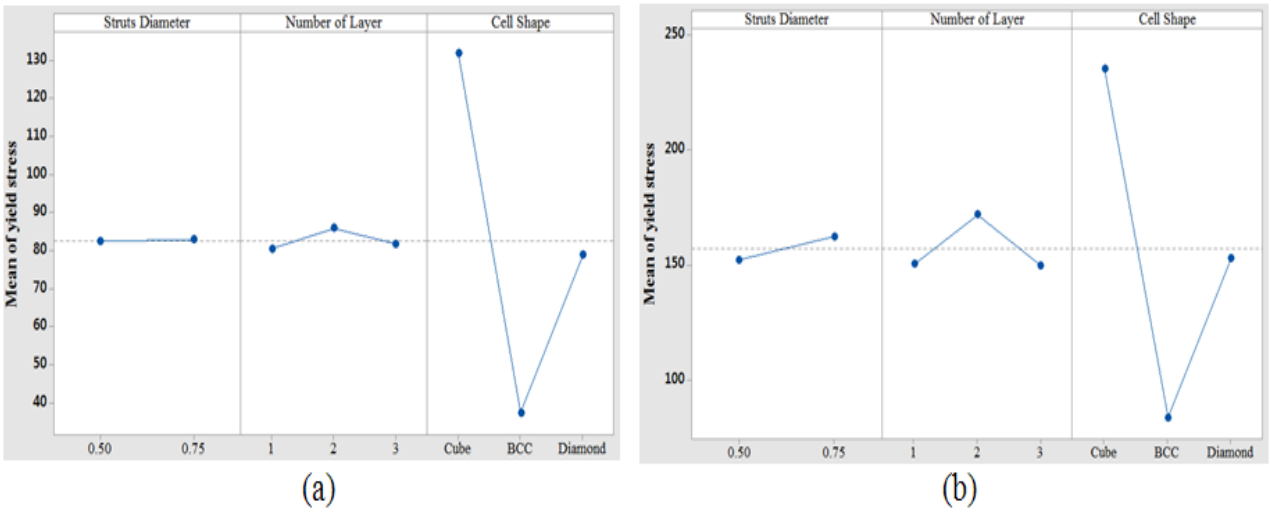

Figure13. Yield strength results` analysis in scaffolds with a) 70% porosity and b) 50% porosity

The produced metal implant of Young's modulus traditionally is much higher than biogenic structures. Therefore, the layer structure of the titanium alloy sample scaffolds, which had been examined in this study, significantly caused a reduction in Young's modulus, compared to dense alloy. It is expected that this would cause a significant reduction in strain-shielding. It is reported that bone compression properties depended on age and inner-body situations [32 – 35]. Compressed strength in cortical bone and cancellous bone was in the range of 100 - 230 MPa and 2 – 12 MPa,

and their Young's modulus was in the range of 3 – 30 GPa and 0.02 – 0.2 GPa [1, 31]. The young's modulus and yield strength amounts in most simulated scaffolds in this study were in the range of amounts, related to the bone [36].

4.4 The Effect of Production Deficiencies on Mechanical Properties

One of the advantages of the numerical approach is the possibility of building models with deficiencies caused by the production process, whereas in other approaches they cannot be easily taken into consideration. Since in additive manufacturing, method parts are built layer by layer in most cases, production deficiencies reoccur in layers, which leads to defective columns in scaffolds and eventually to the reduction in mechanical properties. For example, to examine the numerical method's capability, some certain deficiencies in the middle layer of the L17 scaffold were made (Figure 14) and its mechanical properties, under compression load, were compared to a perfect scaffold. The made deficiency removed a strut from a BCC unit-cell with a size of 2 mm.

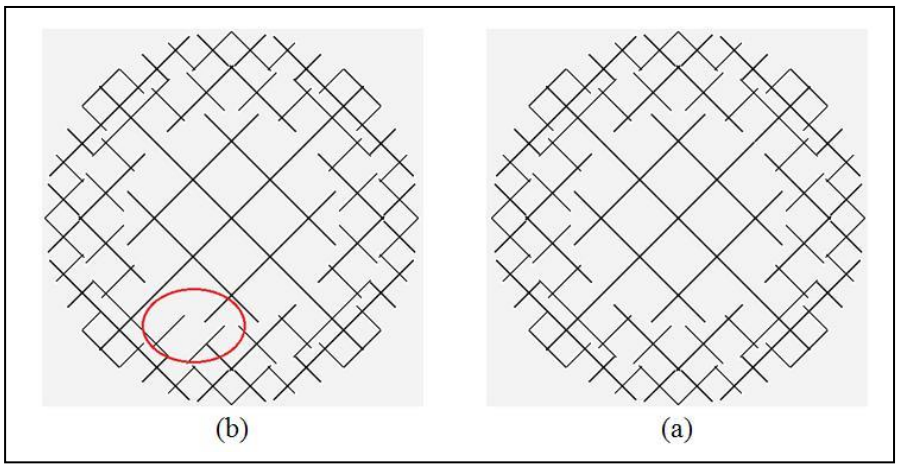

Figure14. Overview of L17 scaffold a) perfect and b) defective

The numerical simulation results of the mechanical properties have been presented in Table 7 and the radial movement of the scaffold's nodes after 3mm loading have been shown in Figure 15. These deficiencies, in addition to reducing the mechanical properties to approximately 1%, caused the separation between the middle layer and the outer layer in the scaffold.

Table7. Mechanical properties of the L17 scaffold perfect and defective

Mechanical properties	scaffold perfect	scaffold defective
Young's modulus	3.09 GPa	3.07 GPa
Yield strength	29.1 MPa	28.86 MPa

5. Conclusion

To show the effect of the number of layers, cell form and strut's diameter on mechanical properties, 36 types of scaffolds with 50% and 70% porosity were designed. The current study verified that mechanical properties of the scaffolds depended less on the number of layers and the unit-cell strut's diameter and the most effective factor was in the unit-cell form. Also according to the presented researches' results in this article, Young's modulus and the yield strength of the

multilayer structure in cubic cells, BCC and diamond made of titanium alloy and with 70% porosity were, respectively, in the range of 1.08 – 18.66 GPa and 31.12 – 148.19 MPa and with 50% porosity, respectively, in the range of 3.09 – 35.42 GPa and 67.2 – 277.14 MPa, which was in the range of amounts related to the bone. These results showed that the titanium alloy-made scaffolds had mechanical properties comparable with human bones, and two-layer scaffolds had higher strength without changing Young's modulus. Also, this advantage was more significant in high-density scaffolds.

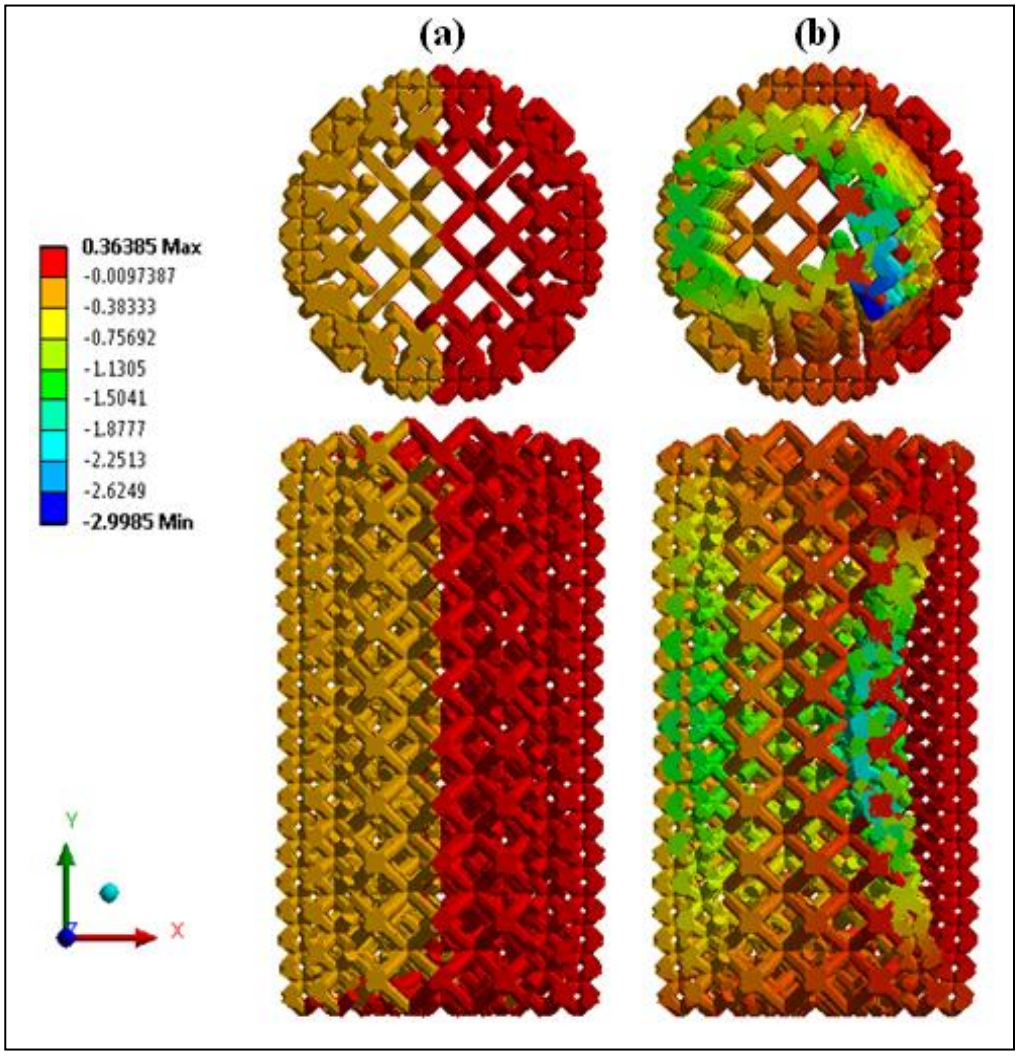

Figure15. longitudinal and cross-section of radial movement of the scaffold's nodes per millimeter after 3mm loading in L17 scaffold a) perfect and b) defective

Conducting a great number of experimental tests on cell scaffolds can be time-consuming and costly. To examine the designs of more scaffolds with altering geometrical parameters, a numerical approach can be taken into account for target amounts in mechanical properties or optimizing the form under the load. Analyzing the limited element can provide the possibility to examine mechanical properties, like structure's modulus, compressed strength and strain distribution in the complex structure for optimizing the clinical applications without using scaffold or destructive

experimental test. Analyzing the limited element can present the effect of deficiencies through models having deficiencies caused by the production process and also precise stress and strain distribution in scaffolds whose experimentally calculating is difficult but useful in optimizing the scaffolds. The conformity between the numerical simulation results and experimental results in the current study verified the model and the numerical method for simulating multilayer scaffolds and can be a suitable tool for conducting studies on multilayer scaffolds.

One of the simplified matters in the numerical simulation in the current study was assuming the isotropic mechanical properties for the substances forming the scaffold, which according to the fact that the model's navigation during building is one of the most important effective factors on mechanical properties, it can be discussed in future researches.

The results of this research can be useful in designing effective implants for bone tissue regeneration and bone growth.

6. References

[1]Wang, X.,Xu, S.,Zhou, S.,Xu, W.,Leary, M.,Choong, P.,Qian, M.,Brandt, M. andXie, Y.M. 2016.Topological Design and Additive Manufacturing of Porous Metals for Bone Scaffolds and Orthopaedic Implants: a review. Biomaterials. 83: 127-141.

[2]Feng, Y. F., Wang, L., Li, X., Ma, Z. S., Zhang, Y., Zhang, Z. Y. and Lei, W. 2012.Influence of Architecture of β-tricalcium Phosphate Scaffolds on Biological Performance in Repairing Segmental Bone Defects. PLOS One. 7(11): 1-12.

[3]Das,S. A. andBotchwey,E. 2011.Evaluation of Angiogenesis and Osteogenesis. Tissue Engineering Part B: Reviews. 17(6): 403-414.

[4] Gérard,C. and Doillon, C.J. 2010.FacilitatingTissue Infiltration and Angiogenesis in a Tubular Collagen Scaffold. Journal of Biomedical Materials Research Part A. 93(2): 615-624.

[5] Tampieri, A.,Celotti, G.,Sprio, S.,Delcogliano, A. andFranzese, S.2001.Porosity-graded Hydroxyapatite Ceramics to Replace Natural Bone. Biomaterials. 22: 1365–1370.

[6]Pompe, W.,Worch, H.,Epple, M.,Friess, W.,Gelinsky, M.,Greil, P.,Hempel, U.,Scharnweber, D. and Schulte, K.2003.Functionally Graded Materials for Biomedical Applications, Materials Science and Engineering: A. 362: 40-60.

[7]Becker, B. and Bolton, J.1997.Corrosion Behaviour and Mechanical Properties of Functionally Gradient Materials Developed for Possible Hard-tissue Applications, Journal of Mater Sci-Mater M. 8: 793–797.

[8] Gibson, L.J. and Ashby, M.F. 1997.Cellular Solids: Structure and Properties, Cambridge University Press.

[9] Luxner, M.H.,Woesz, A.,Stampfl, J.,Fratzl, P. andPettermann, H.E. 2009.A Finite Element Study on the Effects of Disorder in Cellular Structures. ActaBiomaterialia. 5: 381-390.

[10] Parthasarathy, J.,Starly, B., Raman, S. and Christensen, A. 2010.Mechanical Evaluation of Porous Titanium (Ti6Al4V) Struc-tures with Electron Beam Melting (EBM). Journal of the Mecha- nical Behavior of Biomedical Materials. 3: 249-259.

[11] Hedayati, R.,Sadighi, M.,Mohammadi-Aghdam, M. andZadpoor, A.A. 2016.Mechanical Properties of Regular Porous Bio-materials Made from Truncated Cube Repeating unit Cells:

Analytical Solutions and Computational Models. Materials Science and Engineering: C.60: 163-183.

[12] Babaee, S.,Jahromi, B.H.,Ajdari, A.,Nayeb-Hashemi, H. andVaziri, A. 2012.Mechanical Properties of Open-cell Rhombic Dodecahedron Cellular Structures. ActaMaterialia. 60: 2873-2885.

[13] Borleffsm, M. 2012.Finite Element Modeling to Predict Bulk Mechanical Properties of 3D Printed Metal Foams, TU Delft, Delft University of Technology.

[14]Hedayati, R.,Sadighi, M.,Mohammadi-Aghdam, M. andZadpoor, A.A. 2016. Mechanical Behavior of Additively Manufac-tured Porous Biomaterials Made from Truncated Cuboctahedron unit Cells. International Journal of Mechanical Sciences. 106: 19-38.

[15] Shulmeister, V., Van der Burg, M., Van der Giessen, E. and Marissen, R. 1988.A Numerical Study of Large Deformations of Low-density Eastomeric Open-cell Foams. Mechanics of Materials. 30: 125-140.

[16] Warren, W. andKraynik, A. 1997.Linear Elastic Behavior of a Low-density Kelvin Foam with Open Cells. Journal of Applied Mechanics. 64: 787-794.

[17] Zheng, X., Lee, H.,Weisgraber, T.H.,Shusteff, M.,DeOtte, J.,Duoss, E.B., Kuntz, J.D.,Biener, M.M.,Ge, Q. and Jackson, J.A. 2014.Ultralight, Ultrastiff Mechanical Metamaterials, Science. 344: 1373-1377.

[18] Hedayati, R.,Sadighi, M.,Mohammadi-Aghdam, M. andZadpoor, A.A. 2016. Mechanics of Additively Manufactured Porous Biomaterials Based on the Rhombicuboctahedron Unit Cell. Journal of the Mechanical Behavior of Biomedical Materials. 53: 272-294.

[19] Ptochos, E. andLabeas, G. 2012. Elastic Modulus and Poisson's Ratio Determination of Microlattice Cellular Structures by An-alytical, Numerical and Homogenisation Methods. Journal of San- dwich Structures and Materials. 14: 597-626.

[20] Ptochos, E. andLabeas, G. 2012. Shear modulus Determination of Cuboid Metallic Open-Lattice Cellular Structures by Analyt-ical, Numerical and Homogenisation Methods. Journal of Strain. 48: 415-429.

[21] Ahmadi, S.,Campoli, G., AminYavari, S.,Sajadi, B.,Wauthl´e, R.,Schrooten, J.,Weinans, H. andZadpoor, A.A. 2014. Me-chanical Behavior of Regular Open-cell Porous Biomaterials Made of Diamond Lattice Unit Cells. Journal of the Me-chanical Behavior of Biomedical Materials. 34: 106-115.

[22] Hedayati, R.,Sadighi, M.,Mohammadi-Aghdam, M. andZadpoor, A.A. 2016. Effect of Massmultiple Counting on the Elastic Properties of Open-cell Regular Porous Biomaterials. Materials and Design. 89: 9-20.

[23]Bitsche, R.,Daxner, T. andBohm, H.J. 2005. Space-Filling Polyhedra as Mechanical Models for Solidified Dry Foams, TechnischeUniversit at Wien.

[24] Buffel, B.,Desplentere, F.,Bracke, K. andVerpoest, I. 2014. Modelling Open Cell-foams based on the Weaire-Phelan Unit Cell with AMinimal Surface Energy Approach. International Journal of Solids and Structures. 51: 3461-3470.

[25] Kraynik, A.M. andReinelt, D.A. 1996.Linear Elastic Behavior of Dry Soap Foams. Journal of Colloid and interface Science. 181: 511-520.

[26] Surmeneva, M.,Surmenev, R.,Chudinova, E.,Koptioug, A.,Tkachev, M.,Gorodzha, S. andRannar, L.E. 2017.Fabrication of Multiple-layered Gradient Cellular Metal Scaffold via Electron Beam Melting for Segmental Bone Reconstruction. Materials & Design. 133: 195-204.

[27] Daxner, T. 2010.Finite Element Modeling of Cellular Materials. Cellular and Porous Materials in Structures and Processes. Springer: 47-106.

[28] Heinl,P.,Müller, L.,Körner, C.,Singer, R.F. and Müller, F.A. 2008.Cellular Ti-6Al-4V Structures with Interconnected Macro Porosity for Bone Implants Fabricated by Selective Electron Beam Melting.ActaBiomaterialia. 4(5):1536-1544.

[29] Bandyopadhyay, A.F.,Balla, V.K.,Bose, S.,Ohgami, Y. and Davies, N.M.2010. Influence of Porosity on Mechanical Properties and in Vivo Response of Ti6Al4V Implants. ActaBiomaterialia. 6: 1640-1648.

[30] Heimann, R.B.,Hemachandra, K. and Itiravivong, P. 1999.Materials Engineering Approaches Towards Advanced Bioceramic Coatings on Ti6Al4V Implants. Journal of Metals, Materials and Minerals. 8(2): 25-40.

[31] Yavari, S.A.,Wauthlé, R.,Van der Stok, J.,Riemslag, A.C.,Janssen, M.,Mulier, M.,Kruth, J.P.,Schrooten, J.,Weinans, H. andZadpoor, A.A. 2013.Fatigue Behavior of Porous Biomaterials Manufactured using Selective Laser Melting. Materials Science and Engineering: C. 33: 4849-4858.

[32] Tan, X.P.,Tan, Y.J.,Chow, C.S.L.,Tor, S.B. and Yeong, W.Y. 2017.Metallic Powder-bed based 3D Printing of Cellular Scaffolds for Orthopaedic Implants: A Stateofthe Art Review on Manufacturing, Topological Design, Mechanical Properties and Biocompatibility. Materials Science and Engineering C. 76: 1328-1343.

[33] Choi, K.,Kuhn, J.L.,Ciarelli, M.J. and Goldstein, S.A. 1990.The Elastic Moduli of Human Subchondral, Trabecular, and Cortical Bone Tissue and the Size-dependency of Cortical Bone Modulus.Journal of Biomechanics. 23: 1103-1113.

[34] Rho, J.Y.,Kuhn-Spearing, L. and Zioupos, P. 1998.Mechanical Properties and the Hierarchical Structure of Bone.Medical Engineering & Physics. 20: 92-102.

[35]Rho, J.Y.,Ashman, R.B. and Turner, C.H. 1993.Young's Modulus of Trabecular and Cortical Bone Material: Ultrasonic and Microtensile Measurements. Journal of Biomechanics.26: 111-119.

[36] Bayraktar, H.H.,Morgan, E.F.,Niebur, G.L.,Morris, G.E.,Wong, E.K. and Keaveny, T.M. 2004.Comparison of the Elastic and Yield Properties of Human Femoral Trabecular and Cortical Bone Tissue.Journal of Biomechanics. 37: 27-35.